Thermal Radiative Properties of the Microwave Anisotropy Probe Telescope

James B. Heaney[*a], Charles C. He[*a], Wanda C. Peters[*a], Robert R. Gorman[*a], Samuel Dummer[**b], Clifton E. Jackson[***c], John T. VanSant[c]
[a]Swales Aerospace; [b]Surface Optics Corp; [c]Goddard Space Flight Center

ABSTRACT

The twin composite structure telescopes aboard the Microwave Anisotropy Probe were selectively roughened to reduce focused solar radiance. They were then overcoated with evaporated Al + reactively evaporated silicon oxide films whose respective thicknesses were sufficient to achieve the high reflectance (low emittance) of bulk aluminum at the microwave operating frequencies; high emittance in the thermal emittance (300K) region ($\varepsilon > 0.50$); and moderately low solar absorptance ($\alpha < 0.4$) for a resultant $\alpha/\varepsilon < 0.9$. This report will discuss the experimental techniques used to prepare the telescope reflector surfaces and to evaluate their resultant properties.

1. INTRODUCTION

The Microwave Anisotropy Probe (MAP) is a joint NASA/Princeton University spacecraft mission designed to observe the cosmic microwave background radiation at selected frequencies over the 22 – 90 GHz range with better angular resolution (< 0.3° vs. 7°) and sensitivity (~ 20μK per 0.3° pixel) than the earlier Cosmic Background Explorer (COBE, c. 1990)[1,2]. In order to achieve this improved spatial resolution in a full sky survey, MAP will use two essentially identical off-axis Gregorian telescopes arranged back-to-back on a spinning spacecraft in a differential radiometer configuration. See Figures 1a & 1b. The observatory spin rate will be ~ 0.45 rpm with a precession rate of about 1 revolution per hour.

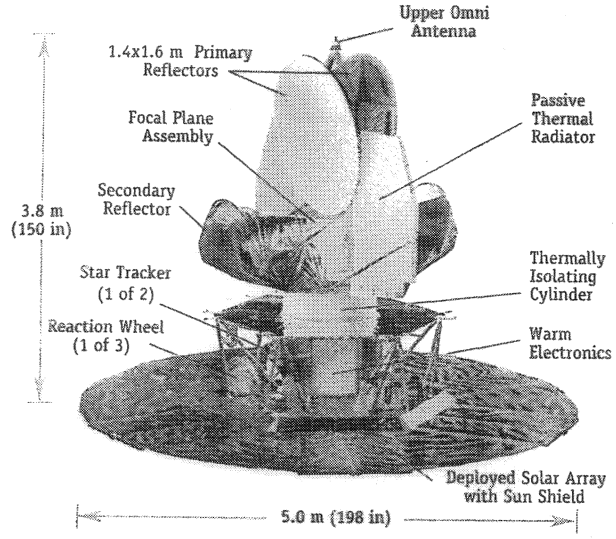

Figure 1a. The MAP spacecraft.

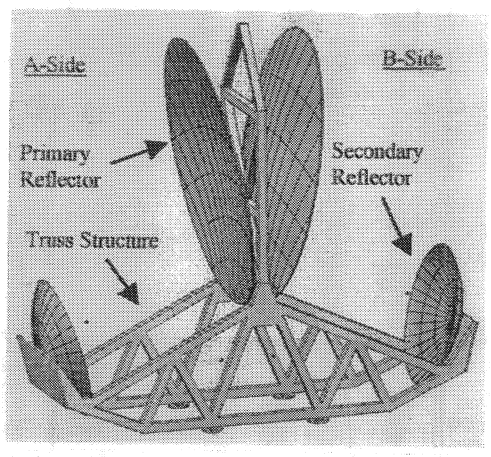

Figure 1b. The MAP telescope and truss structure.

*jheaney@swales.com; Tel: 301-902-4531; Swales Aerospace, 5050 Powder Mill Road, Beltsville, MD 20705; **sdummer@surfaceoptics.com; Tel: 858-675-7404; Surface Optics Corporation, 11555 Rancho Bernardo Road, San Diego, CA 92127; ***cliff.Jackson@gsfc.nasa.gov; Tel: 301-286-6862; Goddard Space Flight Center, Greenbelt, MD 20771.

Optomechanical Design and Engineering 2001, Alson E. Hatheway, Editor,
Proceedings of SPIE Vol. 4444 (2001) © 2001 SPIE · 0277-786X/01/$15.00

Each telescope primary reflector is a 1.6m x 1.4m composite structure, figured as a modified paraboloid, with graphite/cyanate ester face-and back-sheets that sandwich a Korex core. The secondary reflectors are 0.9m diameter modified ellipsoids of the same composite construction as the primaries. Both telescopes are supported on a composite truss structure. The spacecraft will orbit the Sun at the L_2 Lagrange point, about 1.5 x 10^6 km beyond Earth's orbit. With the sunshield deployed and when on station at L_2, the telescopes will operate at a temperature <~50K.

MAP will reach the L_2 location with a lunar assisted trajectory that consists of a series of phased loop approaches to the Moon. During the initial few hours after launch, the temperature challenged composite telescope structures and the microwave feed horns have an opportunity to experience full solar illumination. A reduction of the solar intensity on the secondary reflectors and in the feed horn focal plane areas is accomplished by a selective roughening of the telescope reflector front surfaces. This has the effect of broadening what would otherwise be a smaller spot of intense encircled solar energy on the secondary reflectors and on the microwave feed horn focal plane area. The recommended upper temperature limit for the telescope composite substrates is about 105°C. Passive temperature control of the telescope reflectors is achieved by coating their roughened front surfaces with evaporated aluminum, thick enough to maintain high reflectance, and complementary low emittance, at microwave frequencies, with an additional outer layer of reactively evaporated silicon oxide (SiO_x) to enhance surface emittance in the 20°C to < 100°C range.

This report will discuss the measured scattering characteristics of the roughened reflector surfaces and the solar absorptances and emittances achieved with the Al + SiOx front surface evaporated coatings.

2.0 MAP TELESCOPE REFLECTOR SURFACE PREPARATION

2.1 Reflector Structure & Surface Roughening

The MAP telescope reflectors and supporting truss system are a composite graphite fiber-cyanate ester structure fabricated and assembled by PCI, Inc.[3] See Figure 1b. The structural details and figure verification of this assembly have been reported previously.[4,5]

After fabrication, and prior to mating with the supporting truss structure, the surface of each individual reflector was discreetly roughened by means of a 'grit blasting' technique. The desired degree of roughening was controlled by selecting the grit particle composition or density (Al_2O_3), size (~ 25um), and its impact velocity. The 'grit blaster' was mounted on a numerically controlled machine at an experimentally determined distance from the concave reflector surface. The air pressure in the gun was also optimized experimentally using test samples prior to roughening an actual reflector. These test samples were overcoated with evaporated Al and their bidirectional reflectance (BDR) evaluated in a feedback process in order to arrive at the desired grit blaster settings that could produce surface roughness with the desired degree of expected solar intensity scattering. The imposed MAP requirement stated that not more than 20% of incident sunlight should fall within a 10° half-angle cone after reflection from a roughened primary reflector surface. The results of this roughening process will be discussed below.

The primary reflectors were roughened using a linear step and repeat process by PCI, Inc.[3] using their numerically controlled machine. The smaller size and deeper contour of the secondary reflectors enabled a more desirable rotation of the reflector beneath a similar numerically controlled grit blaster at S.O.C., Inc. [6]

2.2 Reflector Coating with Al + SiOx.

During the early minutes after the launch of the MAP spacecraft, there is a small but finite probablity that the telecopes might acquire a direct view of the sun. This could deliver intense focused sunlight onto the

secondary reflectors and the microwave feed horn focal plane area, prior to deployment and subsequent shadowing provided by the spacecraft sunshield (Figure 1a). Reflector surface roughening, as discussed above, significantly reduced the solar flux per unit area that might reach the secondary reflectors or feed horns.

Temperature control of the MAP telescopes is entirely passive, driven by the solar absorptances (α) of the reflectors' front surfaces and thermal emittances ($\varepsilon(T)$) of their front and back surfaces. The reflector back surfaces are covered with Kapton blanket insulation and there is relatively poor thermal conductance between front and back surfaces through the Korex core material. Consequently, the front surface emittance dominates during the initial launch period of brief solar exposure.

Thermal modeling of the structural integrity of the composite reflector structure indicated that their temperatures should be held below ~ 105C.[7] This imposed an upper limit on the ratio $\alpha/\varepsilon(T)$of <~ 0.9. In order to achieve high microwave reflectance (and corresponding low microwave emittance), the reflector front surfaces are coated with evaporated Al which has an α/ε of ~4.0. Consequently, it was necessary to reduce the α/ε of evaporated Al by adding another layer that would increase its emittance, at the temperatures experienced immediately after launch, without increasing the the absorptance of solar energy or the emittance at microwave frequencies.

It has been demonstrated that Al-coated front surface mirror surfaces can lower their α/ε by adding a layer of reactively evaporated silicon oxide (SiOx).[8] The value of the surface emittance increases with increasing SiOx thickness, whereas the solar absorptance remains almost constant for properly oxidized SiO films that have low absorptance throughout the wavelength region of maximum solar intensity (~300nm to 2500nm). Because the SiOx absorbs strongly at wavelengths around 10μm, near the peak radiant intensity of a 300K Planckian radiator, it can produce a maximum radiating efficiency, i.e. high ε, with minimum film thickness, when deposited onto surfaces that are required to maintain temperatures in the 300K to 370K range. The desire to keep the outer dielectric surface thin is consistent with the MAP's need to maintain high metallic reflectivity at microwave frequencies.

This Al + SiOx process was applied to the roughened composite structure MAP reflectors.

2.2.1 Al Film Deposition

The reflectors are required to exhibit an emissivity within 0.1% of that of bulk aluminum at microwave frequencies $\leq$ 90GHz. In order to achieve bulk-like Al properties with a vapor deposited thin film, it was necessary to guarantee that the Al film was sufficiently thick, yet not so thick that it would be impossible to deposit using the chosen vacuum evaporation process.

From Ref. 9 , the skin depth of Al is given by: $\delta = (1/4\pi)(c\lambda/\mu\sigma)^{1/2} = (1/4\pi)(cr\lambda)^{1/2}$ .....(1)

where μ = magnetic permeability = 1 for Al; c = 3 x 10^{10} cm/sec; r = resistivity of Al; λ = wavelength.

The longest wavelength detected by the MAP receivers is about 13.6mm. For bulk Al at 300K, r = 2.7$\mu\Omega$-cm $\approx$ 3.0 x 10^{-18} sec.[10] Inserting these values into eq. (1) yields a skin depth $\delta \approx$ 0.3 μm. Because the MAP telescopes will operate at a temperature near 40K when on station at L2, the resistivity of Al will decrease by more than two orders of magnitude with the result that the penetration depth will be less than 0.03μm. However, actual measurements performed by M. Halpern have demonstrated that the resistivity of the type of Al thin film deposited onto the MAP reflectors is higher than that of bulk Al at cryogenic temperature, resulting in a somewhat greater skin depth than computed when using values for bulk Al.[11]

Because the graphite fiber/cyanate ester surfaces of the MAP primary and secondary reflectors were intentionally roughened to promote the scattering of solar wavelength radiation, there was a concern that an evaporated Al film of thickness about 0.1μm might be insufficient to insure robust coverage of the heavily

roughened surface. Consequently, the thickness of the Al layer was targeted to be no less than 1.5μm, more than 15 times greater than the expected penetration depth at a temperature of 40K.

In addition, measurements performed by N. Butler on coated MAP reflector samples verified their low emissivity at 90GHz.[12]

The Al film was deposited in a cryo-pumped vacuum chamber at S.O.C., Inc.[6] that was large enough to contain the 1.6m x 1.4m primary reflectors. Al of purity better than 99.999% was used as the source material. The reflector was suspended in the chamber and rotated over the evaporant during deposition. Thickness was monitored real-time during the deposition using a calibrated quartz crystal microbalance (QCM). The correlation of QCM thickness with post-deposition measurements of the Al thickness over a reflector area was calibrated by means of trial evaporations of Al onto test samples that were arranged in the evaporation chamber in a manner that mimicked an actual reflector configuration. Afterward, the Al film thickness deposited into the test samples was measured using a step height profilometer (Dektak).

Al film thickness was not measured on the reflectors themselves. Instead, witness samples were placed in the coating chamber with each reflector and their film thicknesses were measured using step height profilometry afterward. The test sample calibration data were used to provide Al film thickness as a function of axial (primary) or radial (secondary) distance from a reflector center. The results of this process will be discussed below.

2.2.2 SiOx Film Deposition

The same chamber and reflector mount configuration was used for the SiOx deposition as had been used for the Al. SiO source material was reactively evaporated in a partial pressure of oxygen, following the recipe of ref. 8, to produce clear films of SiOx onto evaporated Al that exhibited low solar absorptance. As was done for the Al deposition, trial runs with test samples were used to calibrate the QCM and to establish the distribution of SiOx thickness across each reflector's surface area. The ultimate goal was to produce surfaces with an $\alpha/\varepsilon < 0.9$. This could be achieved on the MAP reflector roughened composite surfaces if the SiOx film thickness was kept in the 2.0um to 2.4um range. Surface emittance is a sensitive function of SiOx thickness as demonstrated in Figures 2a and 2b (ref. 8). (Note that in Figures 2a & 2b thickness is expressed in terms of optical thickness at 550nm, i.e. quarter-waves, λ/4. One λ/4 equals about 88nm of SiOx.)

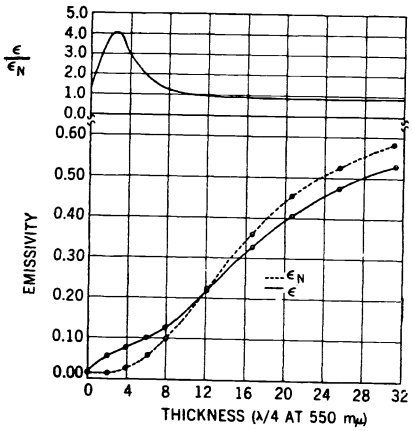

Figure 2a. The hemispherical, ε, and normal, ε_n, emittances and $\varepsilon/\varepsilon_n$ ratio of mirror surfaces coated with Al + SiO_x of various thicknesses. (Ref. 8)

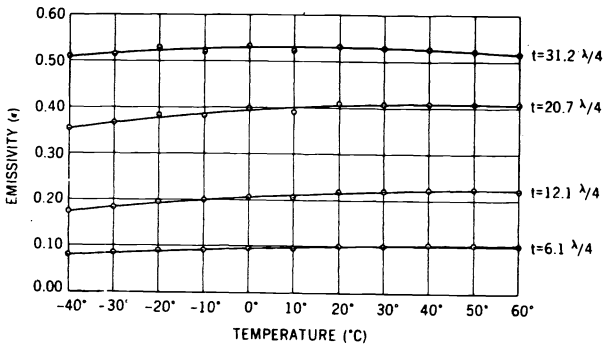

Figure 2b. ε as a function of temperature for mirror surfaces coated with Al + SiOx. (Ref. 8)

Three independent methods were used to determine the thickness of SiOx deposited onto each reflector. (1) Post-deposition contact profilometry on coated witness samples, similar to what was done for the Al deposition, was used to measure the coating physical thickness. (2) Post-evaporation reflectance measurements of the Al + SiOx witness samples that were placed in the chamber during reflector coating were made over the 300nm to 2400nm wavelength range and the maxima and minima in the visible reflectance spectra revealed the SiOx film's optical thickness, as shown in Figure 3.

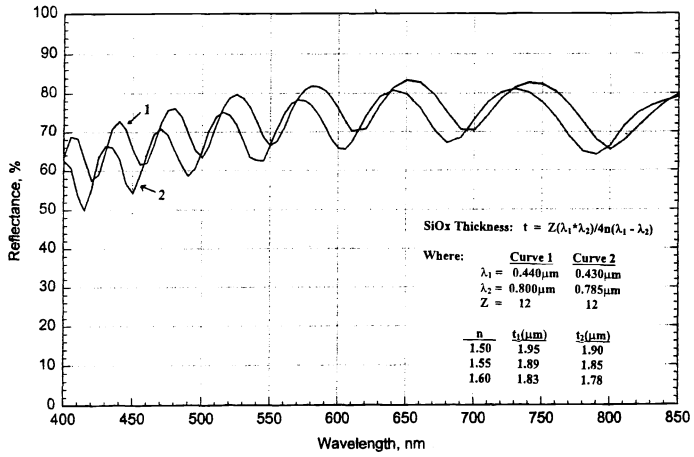

Figure 3. The reflectance of two glass substrate witness samples coated with Al + SiO_x together with a MAP reflector and used to estimate SiO_x thickness.

The physical thickness of the SiOx film can be derived from the optical thickness by assuming a value for the refractive index, n, of the SiOx, and then applying the equation: $Z = (\lambda_1\lambda_2)/4n(\lambda_1 - \lambda_2)$, where Z is the number of maxima and minima in the reflectance spectrum between λ_1 and λ_2, and n is the refractive index of the SiO_x film ($1.50 < n < 1.60$). The results of this calculation are presented in Figure 3. (3) The emittances of witness samples were measured and compared with the emittance vs. thickness data of Figure 2a.

The thickness uniformities of the Al and SiO_x films deposited onto the MAP primary and secondary reflectors, estimated from witness samples subjected to trial evaporations and by applying the above thickness measurement methods, are presented in Figures 4a, -b,-c, -d.

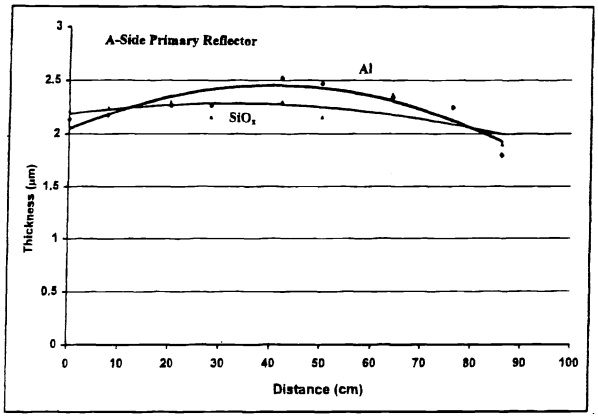

Figure 4a. The Al and SiO_x thickness uniformities for the MAP Side A primary reflector.

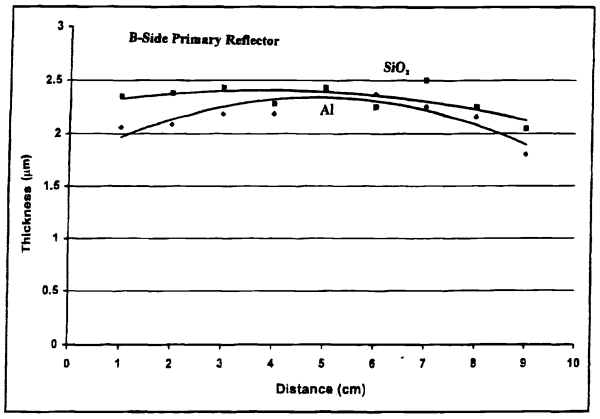

Figure 4b. The Al and SiO_x thickness uniformities for the MAP Side B primary reflector.

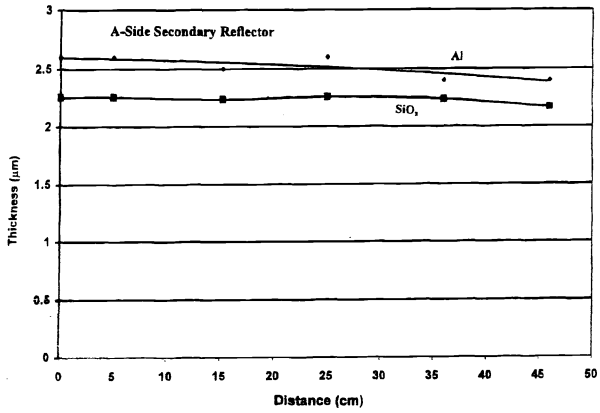

Figure 4c. The Al and SiO_x thickness uniformities for the MAP Side A secondary reflector.

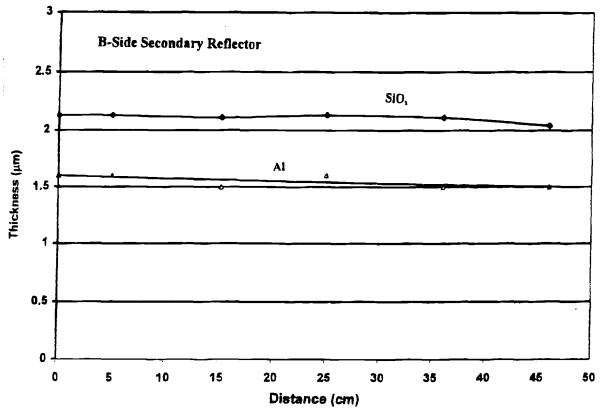

Figure 4d. The Al and SiO_x thickness uniformities for the MAP Side B secondary reflector.

3.0 THERMAL RADIATIVE PROPERTIES: MEASUREMENT TECHNIQUES AND RESULTS

3.1 Surface Roughness and Scattering Measurements

3.1.1 Surface Physical Roughness

The surface roughnesses of the 4 MAP telescope reflectors were estimated from roughness measurements made on test samples of the reflector composite material that were fabricated and grit-blast roughened at the same time as the reflectors. Two measurement techniques were used: (1) a contact profilometer; and (2) an atomic force microscope (AFM).

Repeated measurements on different samples and on different areas of the same sample with both techniques produced rms surface roughness values in the 250nm to 400nm range. The midpoint of the solar spectral intensity occurs at ~ 730nm. Therefore the degree of surface roughness corresponds to ~ roughness/wavelength $\approx$ 0.34 to 0.55. This should be sufficient to produce substantial scattering over most of the solar spectral intensity wavelength range.

An overly rough surface would act as a light trap to produce an undesirably high reflector solar absorptance. Consequently, the immutable act of roughening each reflector surface was aproached gingerly, with the intent of erring on the side of blasting too lightly rather than more heavily, using the test sample data as a guide.

3.1.2 Surface Scatter Determined From Reflectometry

After application of the Al + SiOx films onto the roughened reflector surfaces, the MAP telescope desired that no more than 20% of reflected radiance be contained within a 10° half-angle cone. For the MAP's off-axis Gregorian telescope design, the most intense transfer of solar irradiance into the system would occur when the sun was at an incidence angle of 19° with respect to a primary reflector normal. Consequently, reflectance measurements of surface scatter were made with the test samples oriented 19° to the incident beam.

Two separate measurement techniques were used, but in each case measurements were made at single wavelengths (550nm and 633nm) rather than over the entire solar spectrum, as will be noted below. This measurement limitation generated an effective 'average' measurement of solar scattering ability. Furthermore, measurements were made on small test samples rather than on the reflectors themselves.

The first scattering measurement technique is shown in Figure 5. A nearly parallel beam from a HeNe laser (λ = 633nm) is first directed into detector #1 for a measurement of total incident power. After reflection from the test sample at an incidence angle of ~ 19°, the reflected beam passes through a defining 10° half-angle aperture, then through two lenses that focus the cone onto detector #2. Then, the power scattered into the 10° half-angle cone collection aperture is given by the ratio: (detector#2)/(detector #1)(lens transmittances).

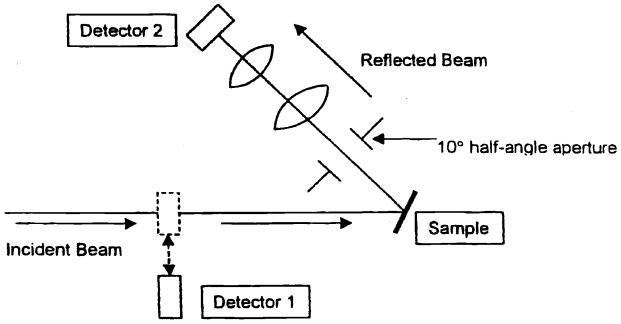

Figure 5. A method for a direct measurement of MAP sample scatter into a 20° cone.

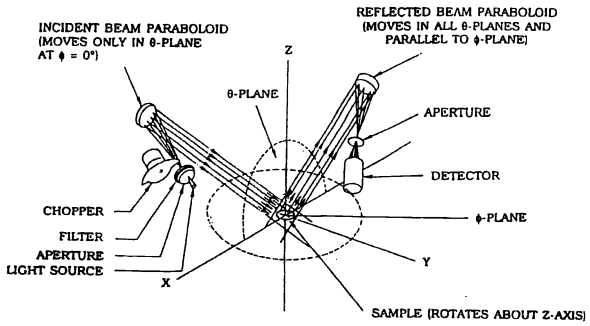

Figure 6. An apparatus for the measurement of MAP sample BRDF.

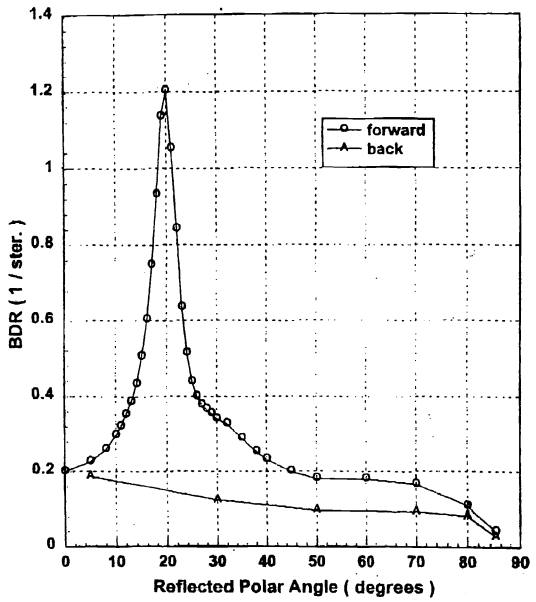

Figure 7. Measured BRDF of a typical MAP witness sample (Side A primary reflector).

This measurement technique produced a measure of the fraction of incident power reflected into a 10° half-angle cone. Dividing this result by the sample's hemispherical reflectance at lambda = 633nm (to be discussed below) yields a reflected scattering value expressed in terms directly applicable to the MAP requirement of less than 20% of reflected, rather than incident, power, to be contained within a 10° half-angle cone.

The second scattering measurement technique employed a bidirectional reflectometer (Surface Optics Corp.) as shown in Figure 6. Radiant power of wavelength 550nm was directed initially onto a near-perfectly diffuse reference surface to establish a reference signal and then onto a coated composite MAP telescope sample at an incidence angle of 19°. The detector was then automatically scanned through the scattering field in the forward and back scattered directions. This method generated bidirectional reflectance data, as shown in Figure 7. Integration of the plotted BRDF data over the desired 10° half-angle cone collection solid angle gave the amount of reflected light into that collection solid angle.

The two scattering measurement techniques gave scattering values for the reflector test samples that were not in perfect agreement, but were more indicative of a scattering trend rather than an absolute measure of expected reflector scattering ability. The measured amount of scattering from the various test samples into a 20° collection cone varied from a low of ~7% for the telescope's Side A primary reflector to a high of ~25% for the Side A secondary reflector.

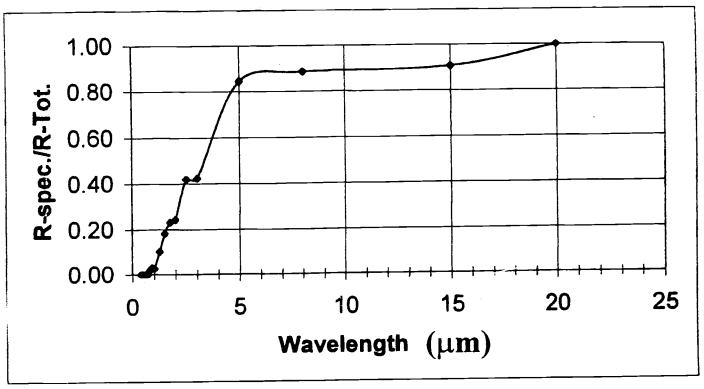

Figure 8. The ratio of specular reflectance to total reflectance of a typical MAP reflector witness sample, measured over the 0.5μm to 20μm wavelength region.

The degree of reflector roughening, i.e. rms roughness in the range 250nm to 400nm, is sufficient to produce a good diffuse scattering surface in the 300nm to 3000nm solar wavelength range, while maintaining near-perfect specularity in the microwave region. This is demonstrated by the reflectance data in Figure 8. An ellipsoidal mirror reflectometer (~2π steradians collection solid angle) that was attached to a Fourier transform spectrometer capable of covering the wavelength range from 2μm to 100μm was used to measure the hemispherical reflectance of a witness sample related to the A-Side primary reflector.

The reflectance of this same sample was then measured using a specular reflectometer (~0.034 steradian collection solid angle) capable of capturing only that portion of the reflected beam contained within this narrow solid angle. The ratio of specular reflectance to total reflectance is plotted in Figure 8 over the 0.5μm - 20μm wavelength range. This plot demonstrates that within the solar wavelength range the degree of specularity is near-zero. I.e., the surface is measurably quite diffuse. Whereas, at wavelengths longer than about 20μm, the total reflectance is entirely specular. The reflectors are essentially perfect mirrors at the MAP instrument operating range, $\lambda > \sim 3$mm.

3.1.3 Scattering Measurements Made on the Assembled Telescope

The test sample bidirectional reflectance measurements described in section 3.1.2 provided evidence that the telescope reflectors were roughened sufficiently to reduce solar concentration on the secondary reflectors and focal plane feed horns. However, it was difficult to use these results to make an accurate prediction of secondary reflector temperature in the event of direct telescope solar exposure in space.

In order to verify analytical predictions of the upper limit of possible secondary reflector temperature due to solar illumination, an actual test of the assembled telescopes was performed with the assistance of L. Page and M. Limon of Princeton University. A tungsten filament stage light, with a slightly divergent output beam, was positioned about 17m from the telescopes and illuminated each primary reflector in turn at an incidence angle of 19°. The spectral output of this lamp, when convolved with the measured reflectance of a typical roughened and coated composite reflector sample, produced an absorptance value that was within 2% of the sample's solar absorptance. That is, an illuminated primary reflector would absorb about as much radiant power from this lamp as it would from the sun. Consequently, a measure of incoming and reflected lamp radiant power with a Si cell detector produced results that were explicitly relevant to secondary reflector temperatures due to solar irradiance.

Data collected from this test was combined with optical ray trace modeling provided by C. Barnes of Princeton Univ. and indicated that the hottest spot on the B-Side secondary reflector would experience slightly more than a one solar constant radiant intensity (~140mw/cm^2) and the A-side secondary would experience about half that. This factor of 2 difference between A- and B-Sides is consistent with the measured bidirectional reflectances of their respective witness samples (7% and 16% respectively into a 20° cone collection angle.)

Thermal modeling of the secondary reflectors indicated that, at this expected solar flux level, reflector surface temperatures would not exceed 105°C in the worst case.[14]

3.2 Solar Absorptance, α, and Thermal Emittance, ε(T), Measurements

The solar absorptance and thermal emittance of each reflector's front surface was estimated from reflectance measurements made on witness samples in order to avoid harmful contact with the reflector surfaces. Coated composite pieces trimmed from reflector edges, that had been roughened and coated together with the reflectors, were also measured and gave results that were in excellent agreement with witness sample measurements.

Measurements of spectral reflectance, ρ_λ, were used to generate the data from which α and ε(T) were derived. The general defining expressions for α and ε(T) are given below.

$$\alpha = 1 - \int_{0.3\mu m}^{7\mu m} (\rho_\lambda J_\lambda)\, d\lambda \;/\; \int_0^\infty J_\lambda\, d\lambda \qquad \varepsilon(T) = 1 - \int_{2\mu m}^{50\mu m} (\rho_\lambda E_\lambda(T))\, d\lambda \;/\; \int_0^\infty E_\lambda(T)\, d\lambda \qquad \ldots\ldots (2)$$

J_λ is the solar spectral irradiance function and $E_\lambda(T)$ is the black body spectral irradiance function for an object at temperature T.

Witness sample spectral reflectances were measured over the 200nm to 2500nm wavelength range using an integrating sphere reflectometer attached to a spectrophotometer. These data were augmented with reflectance data measured over the 2μm to 50μm wavelength range using a combined ellipsoidal mirror hemispherical reflectometer and Fourier transform spectrometer. The reflectance data were then weighted by the solar spectral irradiance function to produce a solar reflectance ρ_S. Then $\alpha = (1 - \rho_S)$.

The reflectance of a typical reflector witness sample (Side B secondary) measured over the 250nm to 2500nm region is presented in Figure 9. The solar absorptance computed for this sample is α = 0.33.

Two measurement methods were used to determine ε(T=300K) from measured witness sample reflectances. The first method used the ellipsoidal reflectometer with Fourier transform spectrometer to measure reflectance over the 2μm to 50μm wavelength band at selected incident angles over the near-normal to 80° range. This measured wavelength band encompasses about 97% of the radiance from a 300K black body. Directional hemispherical reflectance was obtained by integrating the measured reflectances

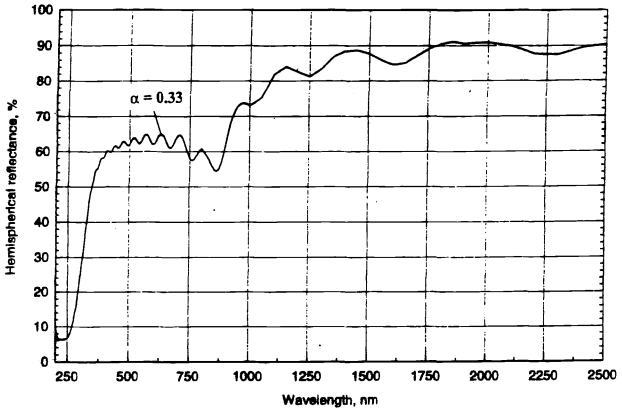

Figure 9. The measured reflectance of a typical MAP reflector witness sample over the 250nm to 2500nm solar wavelength band.

A diagram that illustrates the concept of directional reflectance is shown in Figure 10. Equation 3 expresses the directional reflectance in terms of the measured angular parameters and the incident, N_i , and reflected, N_r , radiant power.

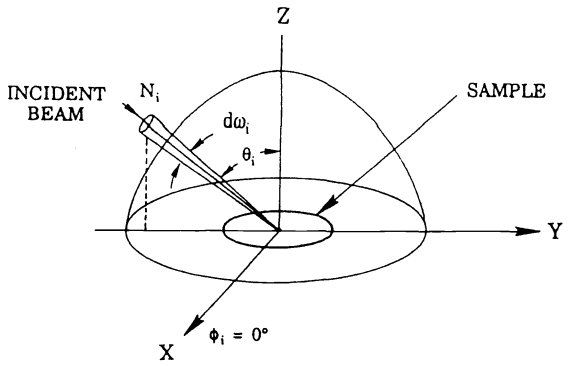

$$\rho_d(\theta_i,\phi_i) = \frac{\int_0^{2\pi}\int_0^{\pi/2} N_r \sin\theta_r \cos\theta_r \, d\theta_r \, d\phi_r}{N_i \sin\theta_i \cos\theta_i \, d\theta_i \, d\phi_i} \quad \ldots..(3)$$

Figure 10. Illustration of the concept of directional reflectance.

Insertion of $\rho_d(\theta,\phi,\lambda)$ into eq. (2) produced the desired value of ε.

The second method used a Gier-Dunkle DB-100[15] portable infrared reflectometer to obtain a rapid measure of reflectance automatically weighted for a 300K black body spectrum at near-normal incidence. Then, near-normal emittance, $\varepsilon_n(300K) = 1 - \rho_n(300K)$. Conversion from near-normal to hemispherical emittance is accomplished with the aid of Figure 2a. For measured $\varepsilon_n(300K)$ values near 0.50 (corresponding to SiOx thicknesses of about 2.1μm, the typical MAP reflector thickness), the ratio $\varepsilon_n/\varepsilon$ is ~1.08. This second rapid method produced ε values that were in excellent agreement with those generated with the ellipsoidal reflectometer.

A comparison of the Gier-Dunkle DB-100 ε_n values with the SiO_x ε_n data of Figure 2a was a final consistency check of the various methods used to obtain the hemispherical emittance of the MAP reflectors' front surfaces.

ε as a function of distance from a reflector center was then adjusted for SiO_x thickness variations across a coated reflector, as discussed in section 2.2.2. The α of SiO_x coated Al is not a sensitive function of SiO_x thickness as demonstrated in Figure 11 (Ref. 8).

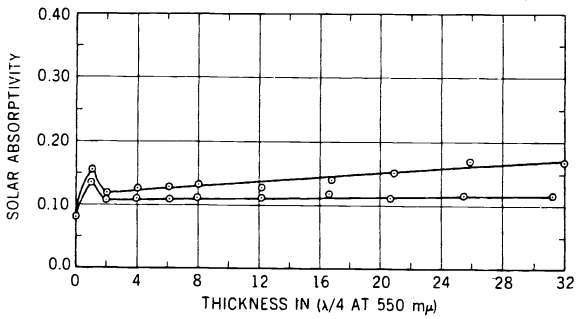

Figure 11. The solar absorptance of partially- and fully-oxidized SiO_x films on Al as a function of film thickness. (1 $\lambda/4 \approx 88$nm).

A typical MAP reflector's SiO_x thickness of 2.0μm to 2.4μm would correspond to about 22 $\lambda/4$ to 28 $\lambda/4$, as expressed in Figure 11. The upper curve in the figure corresponds to an SiO_x film that is experiencing continued oxidation. The lower curve more nearly represents the MAP reflectors' SiO_x film.

The infrared reflectance of a typical MAP reflector witness sample (Side B primary), measured relative to a smooth gold mirror using a specular reflectometer, is presented in Figure 12 over the 2μm to 100μm wavelength region. The collection solid angle of this specular reflectometer is about 0.034 steradian. Consequently, the measured relative reflectance at wavelengths shorter than about 25μm - 30μm is lower than a measure of absolute hemispherical reflectance, as defined by equation (3). However, at wavelengths longer than about 60μm, the reflectance of the MAP reflector witness sample is indistinguishable from that of a smooth mirror surface coated with evaporated gold.

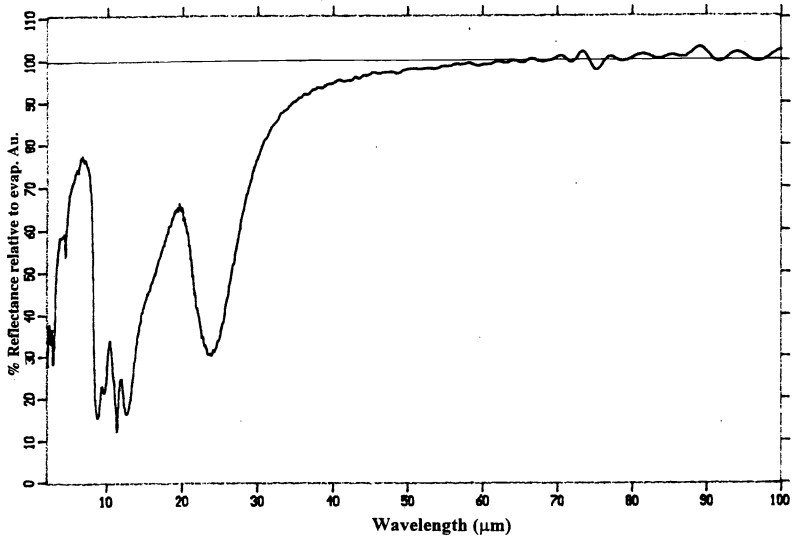

Figure 12. The reflectance of a typical MAP reflector witness sample, measured relative to a smooth evaporated Au mirror using a specular reflectometer, over the 2μm to 100μm wavelength region.

The reflectance data of Figure 12 were augmented with ellipsoidal mirror reflectometer data for wavelengths between 2μm and 25μm and then inserted into equation (2) to generate ε (T) values over the 40K to 370K temperature range.

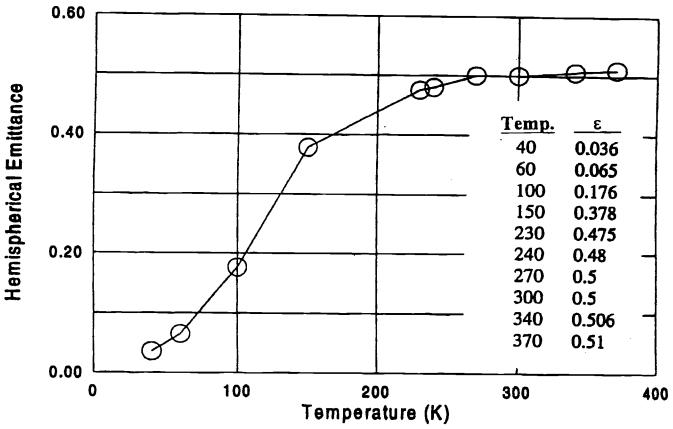

Figure 13. The computed hemispherical emittance of a typical MAP reflector front surface over the 40K to 370K temperature range.

The MAP telescopes are expected to operate in orbit at temperatures approaching 40K, but may experience temperatures as high as about 370K, if a direct view of the sun is acquired in the brief period between launch and full interjection of the sunshade. This computation of ε (T) was aided by the data in Figure 2b over the 230K to 330K range (-40C to + 60C). The computed results are presented in Figure 13 where the ε of a typical MAP reflector is plotted as a function of T over the 40K to 370K temperature range.

In the relatively narrow microwave region over which the MAP instruments operate, ~3mm to ~13mm, the weighting function for a 40K black body inserted into equation (2) would operate on a near-100%

reflectance to yield an effective ε near-zero for the MAP reflector surfaces.

The variation of the MAP reflectors' thermal radiative properties, α/ε and ε , as a function of location on these relatively large coated surfaces is tabulated in Table 3.2-1. The variation of α/ε and ε with distance from a reflector center depends almost entirely on the SiO_x film thickness. Figure 11 demonstrated that α is essentially independent of the SiO_x thickness, whereas the value of ε (T = 300K) is established primarily by the thickness of the SiO_x layer, as presented in Figures 2a and 2b. The emittance of the evaporated Al layer (~0.02) and the surface roughness also make minor contributions to surface emittance for temperatures in the 270K to 370K range. For colder temperatures, the Planckian weighting function of equation (2) shifts to longer wavelengths with the result that surface roughness is much less significant as the ratio of roughness/wavelength decreases and the reflectors become increasingly more specular. The solar absorptance of the Al layer and the surface roughness combine to influence the surface's value of α, but these are generally invariant across a reflector surface.

	MAP Side A Primary		MAP Side B Primary	
Distance From Center (cm)	α/ε	ε	α/ε	ε
0	.73-.81	0.51	0.78	0.51
7.5	.73-.81	0.51	0.78	0.52
20	.72-.80	0.52	0.77	0.52
28	.74-.82	0.50	0.78	0.51
42	.72-.80	0.52	0.77	0.52
50	.74-.82	0.50	0.79	0.51
64	.71-.79	0.52	0.75	0.53
76	.76-.84	0.49	0.79	0.51
84	.88-.98	0.42	0.85	0.47

	MAP Side A Secondary		MAP Side B Secondary	
Distance From Center (cm)	α/ε	ε	α/ε	ε
0	0.76	0.50	0.69	0.49
4	0.76	0.50	0.69	0.49
15	0.76	0.50	0.69	0.49
28	0.76	0.50	0.69	0.49
43	0.76	0.50	0.69	0.49
45	0.78	0.49	0.71	0.48

Table 3.2-1 The variation of MAP reflector thermal radiative properties across the reflector surfaces.

The data in Table 3.2-1 indicate that the MAP reflectors have α/ε values < 0.9, except for the very edge of the Side A primary that is the roughest of the 4 reflectors. The spread in measured α/ε for the Side A primary reflector is caused by both the variation in ε with SiO_x thickness and the uncertainty imbedded in the measurement of α due to the influence of this reflector's surface roughness.

The final value of α/ε or ε listed in the Table was measured on a witness sample placed just beyond a reflector's edge during the coating process. It is only the witness samples that are measured. Their measured reflectances are used to compute α and ε values, as discussed above, that are attributed to the entire reflector, using the coating uniformity data of Figures 4a,-b,-c,-d.

4.0 REFLECTOR COATING DURABILITY

4.1 Coating Aging

The reflectance of witness samples that were coated at the same time as each MAP reflector were monitored periodically, over the 250nm to 2500nm wavelength range, from the date of coating until about two weeks before the MAP launch on 6/30/01. These samples had accompanied the reflectors throughout their pre-launch storage, assembly, and functional and environmental test episodes and experienced the same environmental exposures as the reflectors.

Table 4.1-1 below gives the coating date for each reflector and defines the duration of terrestrial exposure.

REFLECTOR	COATING DATES
Side A Primary	January 1999
Side A Secondary	February 2000
Side B Primary	February 1999
Side B Secondary	February 2000

The measured solar absorptances of all reflector witness samples showed no increase, from the date of coating until immediately before launch, that might indicate a darkening of the surface coating. In the case of the primary reflectors, the pre-launch period was about 29 months.

Table 4.1-1 MAP reflector coating dates.

4.2 Reflector Coating Quality Verification Tests

4.2.1 Coating Adhesion

When each reflector was removed from the coating chamber after the deposition of its outer SiO_x layer, an accompanying witness sample was subjected to, and passed, a standard 'tape' pull test. In addition, this same test was later applied to 'tooling ball tabs' that were an integral part of a coated reflector's outer edge. All 4 reflectors passed this test. This tape pull test was not applied to the usable surface area of any reflector.

In addition, selected witness samples were rapidly immersed in liquid nitrogen for a few minutes and again subjected to a tape pull test. All passed this extreme test.

During photogrammetry shape testing of the reflectors, the retro-reflecting targets were adhered to the reflectors' surfaces using Scotch brand 'Post-It Note' paper adhesive. These were removed, after the assembled MAP telescope had been thermal cycled over the ~90K to 297K temperature range, without harming the surface Al + SiO_x coating.

4.2.2 Humidity Exposure

MAP reflector witness samples experienced a controlled exposure to a 60% relative humidity environment, at a temperature of 30C, for 170 hours. They then were subjected to, and passed, a tape pull coating adhesion test. They also exhibited no measurable change in reflectance in the 250nm to 2500nm region.

4.2.3 Thermal Cycling Tests

The MAP witness samples were also exposed to 12 temperature cycles between 300K and 40K and an additional 12 cycles between 388K and 90K. Once again, they were subjected to and passed a tape pull adhesion test.

The samples were then placed in an evacuated container that was immersed in liquid nitrogen (77K) for 60 days. They passed a tape pull test afterward.

There was no evidence of spontaneous coating delamination after any of these temperature cycling exposures.

The MAP reflectors themselves experienced thermal cycling during photogrammetric shape testing and separate thermal cycling tests. A summary of the temperature ranges to which the reflectors were exposed is contained in Table 4.2.3-1. In all cases, the coated surfaces emerged unharmed.

REFLECTOR	PHOTOGRAMMETRY TESTS	THERMAL VACUUM TESTS
Side A Primary	90K to 270K	138K to 364K
Side A Secondary	n.a.	123K to 362K
Side B Primary	90K to 270K	138K to 364K
Side B Secondary	n.a.	117K to 364K

Table 4.2.3-1 Temperature ranges experienced by the MAP reflectors during pre-launch testing.

5.0 CONCLUDING COMMENTS

- Roughening the graphite fiber + cyanate ester MAP reflector composite face sheets with a grit blasting technique produced surfaces that could reduce solar flux intensity on the telescope secondary reflectors and focal plane areas to an acceptable level.

- Overcoating the roughened reflector surfaces with a layer of evaporated Al thicker than ~1.5μm, plus an outer layer of reactively evaporated silicon oxide (SiO_x) in the 2.0μm to 2.4μm thickness range, produced surfaces that would absorb less than 40% of incident solar irradiation and emit with ~50% efficiency at temperatures in the 300K to 370K range, and therefore not exceed an upper design limiting temperature of ~ 105C due to an incidental direct solar exposure in the early post-launch period, before deployment and interjection of the MAP sunshade.

- The Al + SiO_x surface coating proved to be durable during more than 2 years of terrestrial storage and pre-launch exposure to simulated orbital vacuum and temperature conditions.

6.0 ACKNOWLEDGMENTS

The authors wish to acknowledge the substantial assistance and guidance in the conduct of this effort provided by the MAP project scientist, Dr. Charles Bennett of the Goddard Space Flight Center, the optics lead scientist, Dr. Lyman Page, and the Princeton University Instrument Team of Michele Limon, and Chris Barnes, Dr. Mark Halpern of the University of British Columbia, the Goddard Space Flight Center's Engineering Materials Branch staff, the project direction provided by Goddard's Liz Citrin, the thermal modeling effort led by Goddard's Stuart Glazer, and Acey Herrera, Bruno Munoz, Alan Crane, and Dave Neuberger of Swales Aerospace for multiple contributions in all areas of the reported test program.

REFERENCES

1. See http://map.gsfc.nasa.gov/
2. Tim Folger, "The Magnificent Mission", *Discover Magazine*, pp. 44 ff, May 2000.
3. Programmed Composites, Inc., Anaheim, CA 92807.
4. M.D. Hill, H.P. Sampler, A. Herrera, J.A. Crane, E.A. Packard, and C.G. Aviado, "Alignment measurement of the Microwave Anisotropy Probe (MAP) in the thermal/vacuum chamber using photogrammetry", *SPIE Vol. 4131 – Infrared Spaceborne Remote Sensing VIII,* San Diego, 2000.
5. H.P. Sampler, M.D. Hill and P.D. Mule, "Photogrammetrically measured distortions of composite structure microwave reflectors at ~ 90K", *SPIE Vol. 4131 – Infrared Spaceborne Remote Sensing VIII,* San Diego, 2000.
6. Surface Optics Corporation, 11555 Rancho Bernardo Road, San Diego, CA 92127.
7. Stuart Glazer, private communication, NASA Goddard Space Flight Center, Greenbelt, MD 20771.
8. A.P. Bradford, G. Hass, J.B. Heaney, and J.J. Triolo, "Solar Absorptivity and Thermal Emissivity of Aluminum Coated with Silicon Oxide Films Prepared by Evaporation of Silicon Monoxide", applied Optics, 9, pp 339-344, 1970.
9. M. Born & E. Wolf, *Principles of Optics, 6th Ed.*, Sect. 13.1, Pergamon Press, New York, 1980.
10. *CRC Handbook of Chemistry and Physics, 72nd Ed.*, D.R. Lide, Editor, Sect. 12, Chemical Rubber Publishing Co., Boston, 1992.
11. M. Halpern, Univ. of British Columbia, private communication.
12. N. Butler, "Emissivity Measurements of MAP Satellite Optics", Senior Thesis, Princeton Univ., 1998.
13. C. Barnes, Princeton University, private communication.
14. Stuart Glazer and David Neuberger, private communication, NASA Goddard Space Flight Center, Greenbelt, MD 20771.
15. K.E. Nelson, E.E. Luedke, and J.T. Bevans, "A Device for the Rapid Measurement of Total Emittance", *Journal of Spacecraft and Rockets, Vol. 3*, pp. 758-760, May 1966.